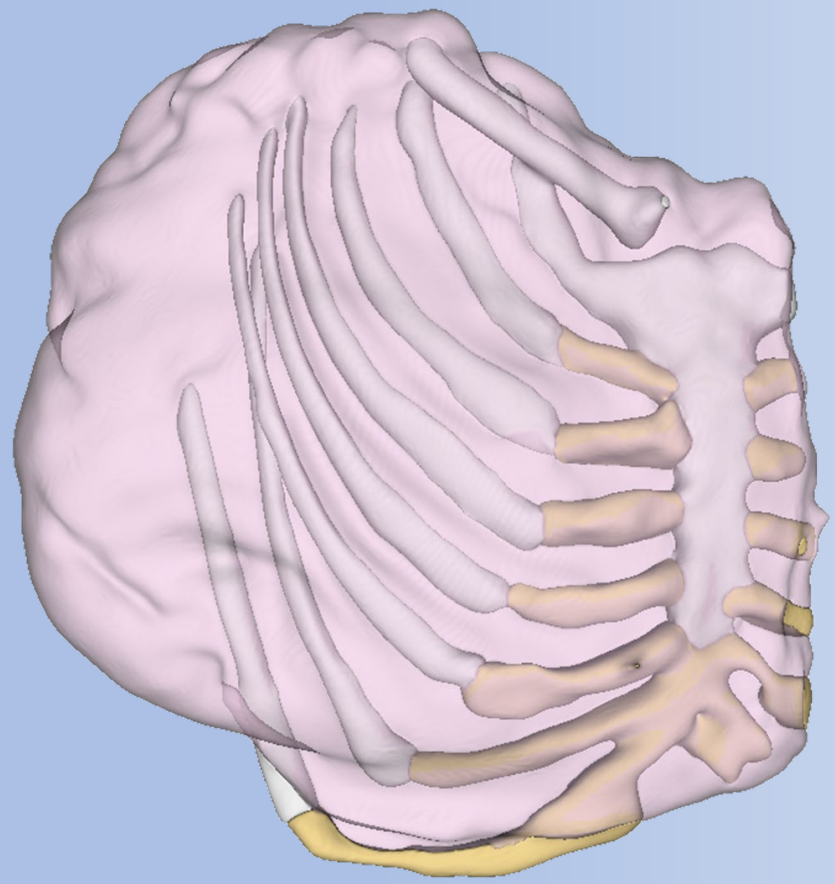

Breast segmentation

FE-based Heterogeneous Digital Volume Correlation to Measure Large Deformations of Breast's Soft Tissues

T. Lavigne, A. Mazier, A. Perney, S.P.A Bordas, F. Hild, J. Lengiewicz

European Commission
école normale supérieure paris–saclay
UNIVERSITÉ DU LUXEMBOURG
LMPS
université PARIS-SACLAY
RAINBOW
Rapid Biomechanics Simulation for Personalized Clinical Design
A Marie Skłodowska-Curie European Training Network
ANATOSCOPE
Legato Team

Context

Preoperative imaging

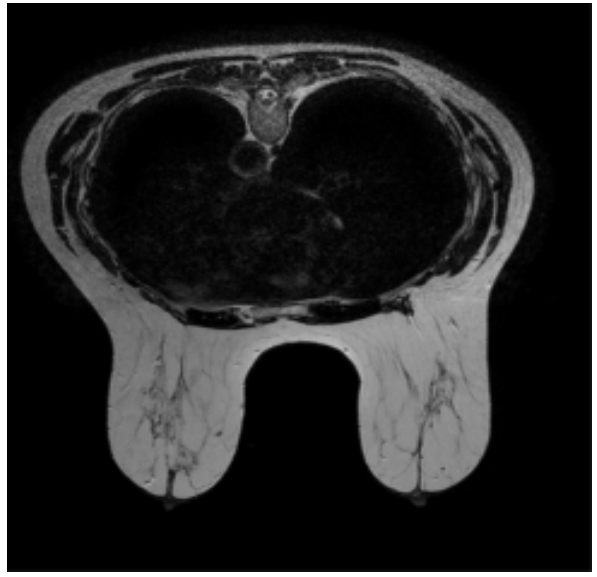

Context

Preoperative imaging

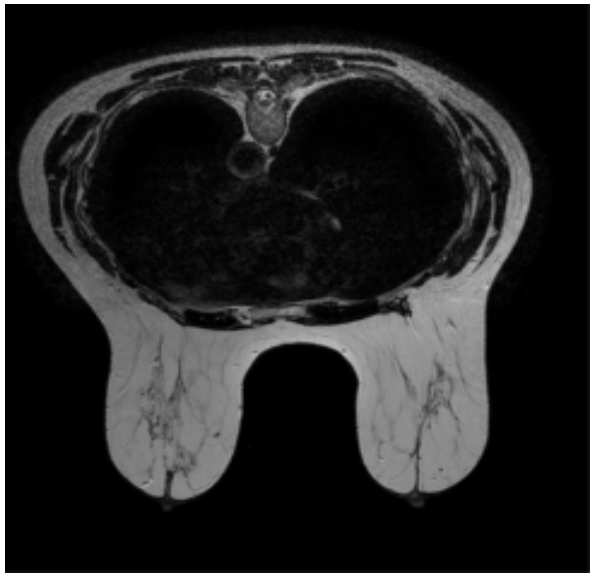

Surgery

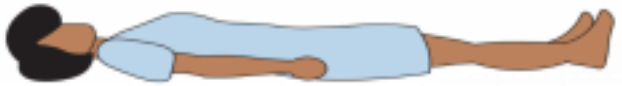

[Gavaghan et al., 2008; Lee et al., 2010; Eiben et al., 2016; Mazier et al., 2021]

Context

Preoperative imaging → **Tumor localization** → **Surgery**

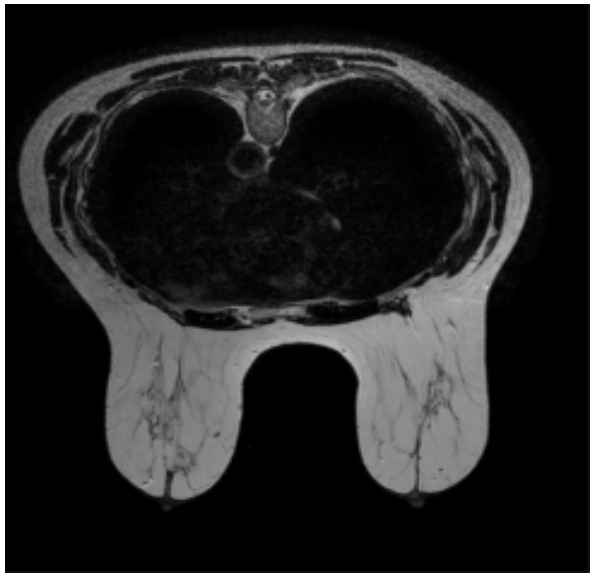

[Duraes et al., 2019]

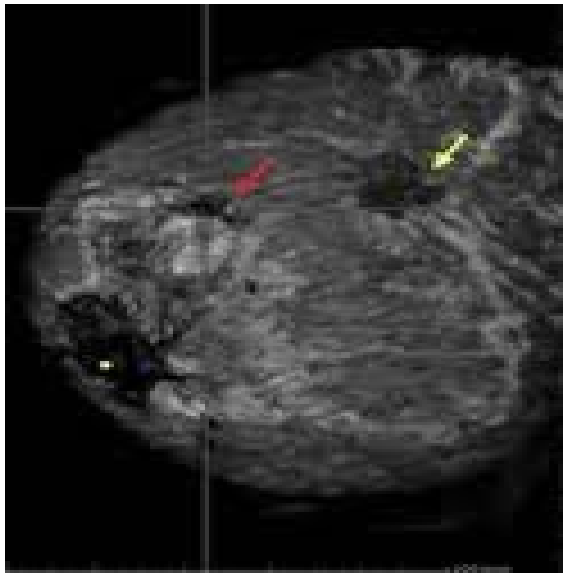

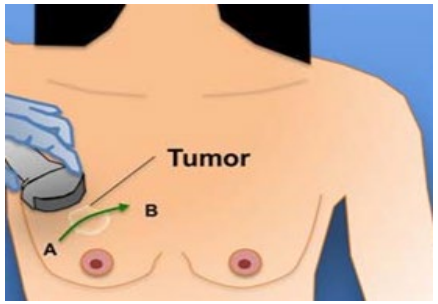

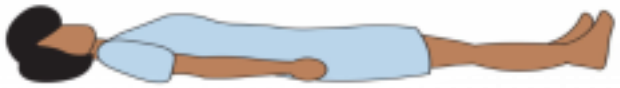

Objective

Predict the deformation from one configuration to another

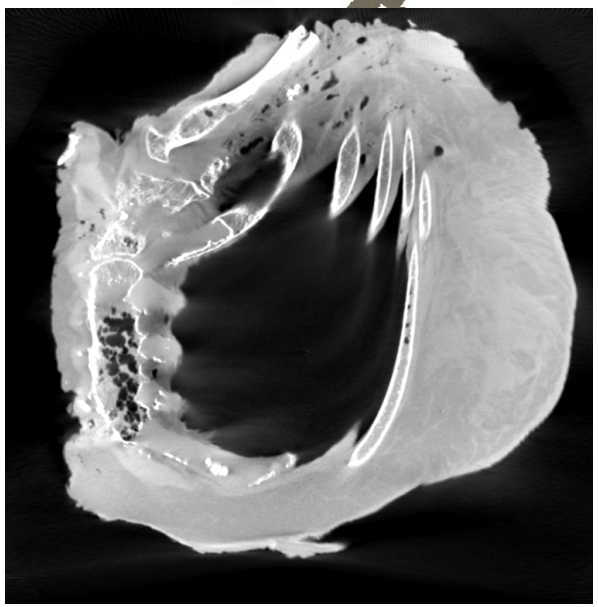

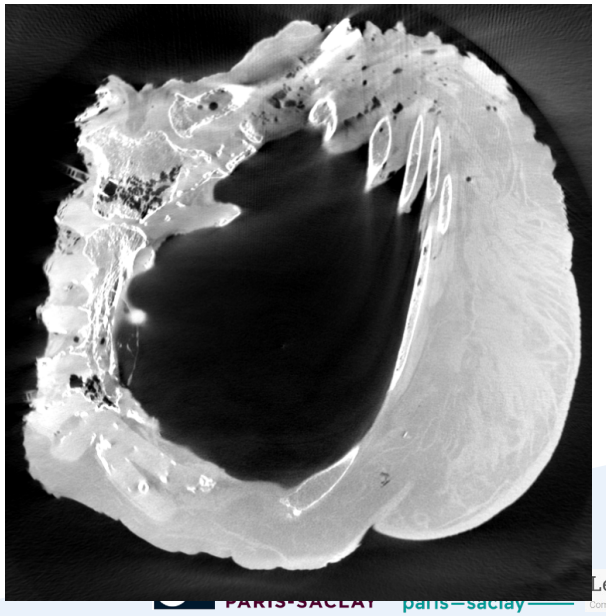

Objective

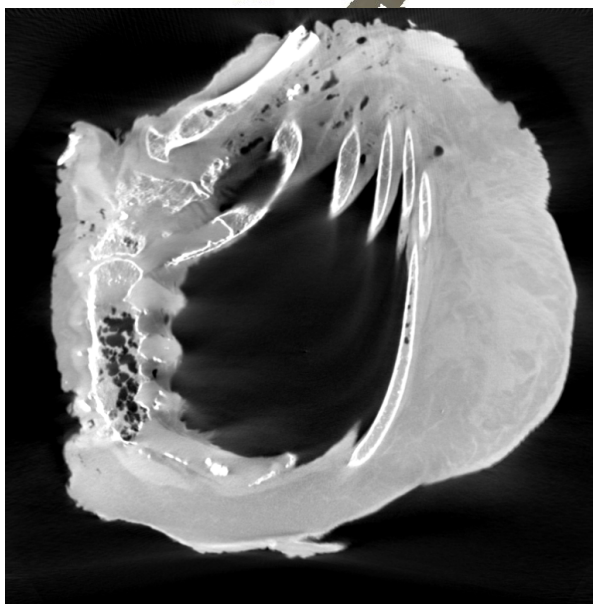

Predict the deformation from one configuration to another

- Measure the full displacement field [Lavigne et al., 2022]

(FE-Based regularized DVC)

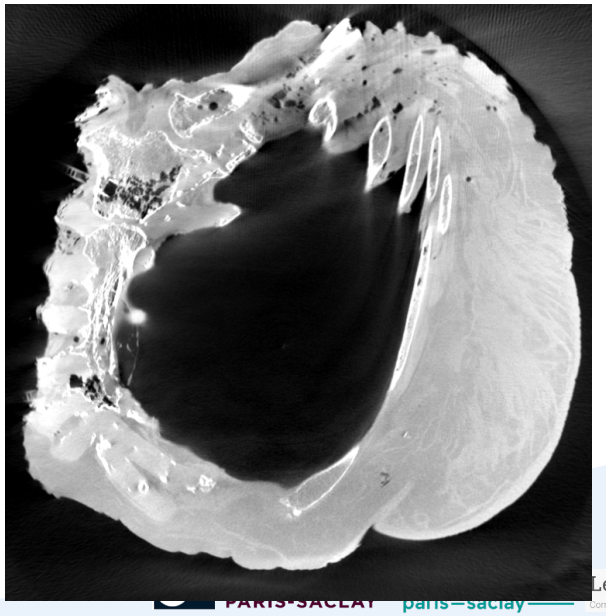

Objective

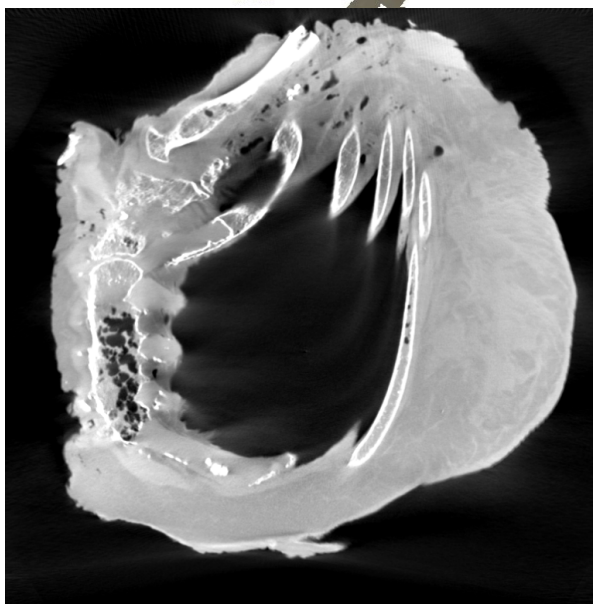

Predict the deformation from one configuration to another

- Measure the full displacement field [Lavigne et al., 2022]
- Identify the patient-specific material properties [Lavigne et al., 2022]

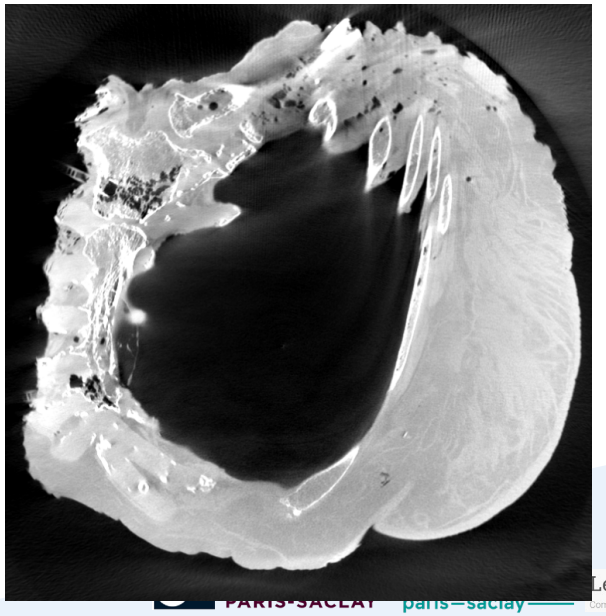

Objective

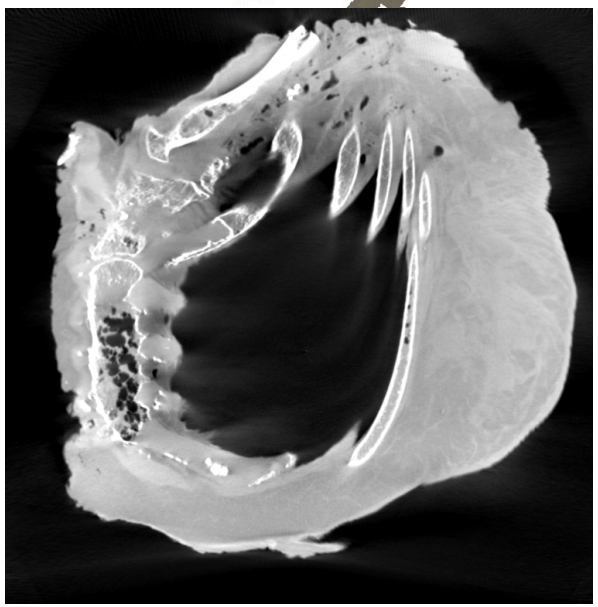

Predict the deformation from one configuration to another

- Measure the full displacement field [Lavigne et al., 2022]
- Identify the patient-specific material properties [Lavigne et al., 2022]
- Surrogate model to obtain real-time predictions for any configuration [Deshpande et al., 2022]

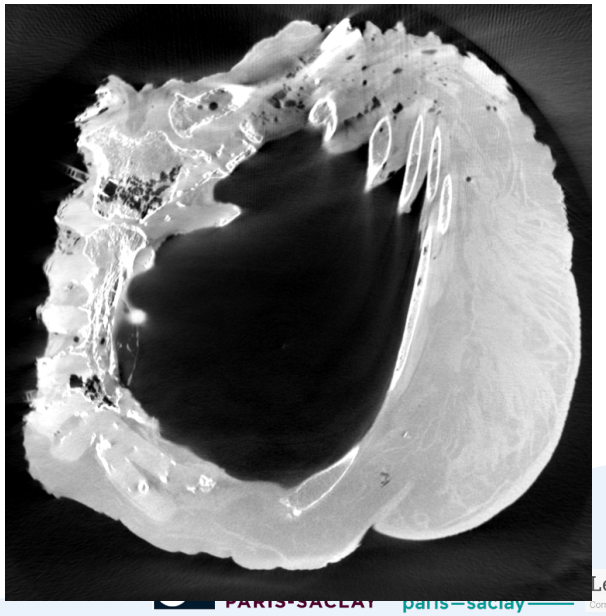

Material and Methods

- Female left **quarter of thorax** injected with physiological serum **attached to a wooden plate** with **4 plastic bands**

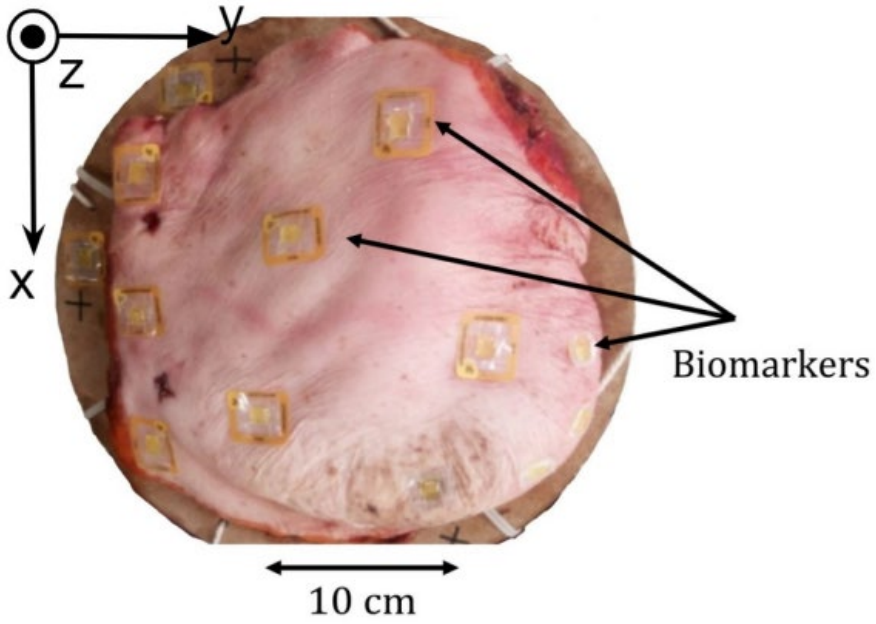

[Lavigne et al., 2022]

Material and Methods

- Female left **quarter of thorax** injected with physiological serum **attached to a wooden plate** with **4 plastic bands**
- **15 biomarkers** (in yellow) on the surface and inside the volume

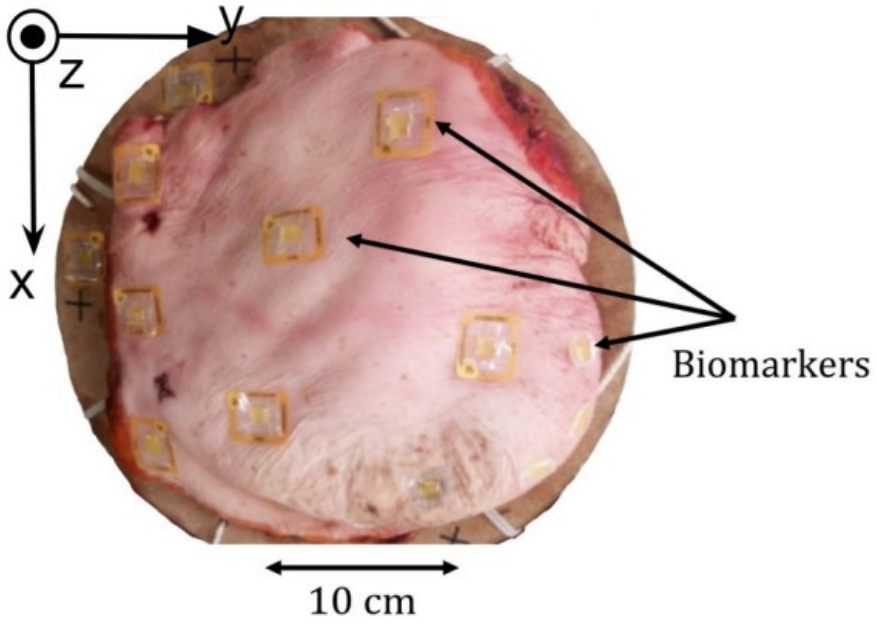

[Lavigne et al., 2022]

Material and Methods

- Female left **quarter of thorax** injected with physiological serum **attached to a wooden plate** with **4 plastic bands**
- **15 biomarkers** (in yellow) on the surface and inside the volume
- **Micro-computed tomography** with an RX Solutions machine (0.34 mm resolution)
- Acquisition in **multiple orientations**.
  Study deals with **-60°** and **-45°** in the axial plane

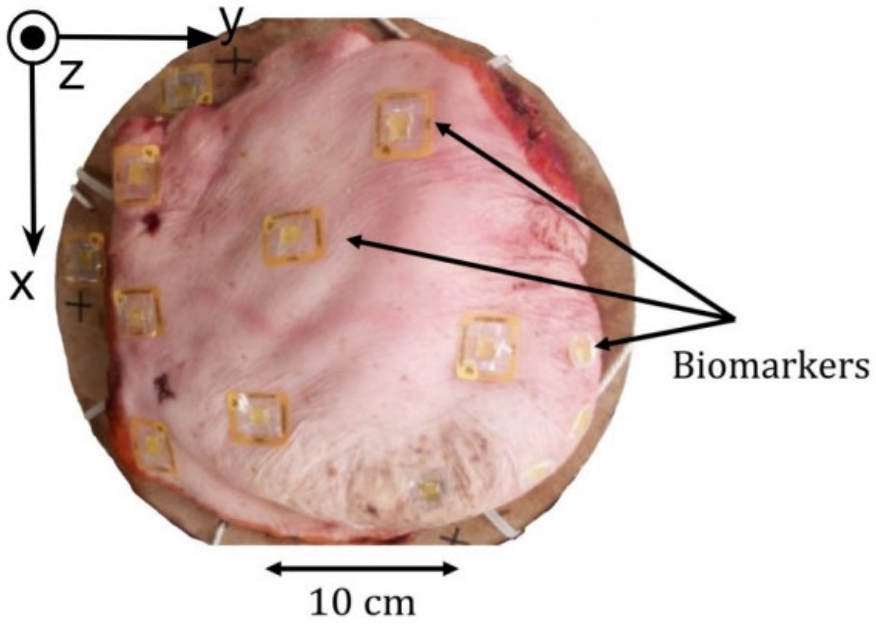

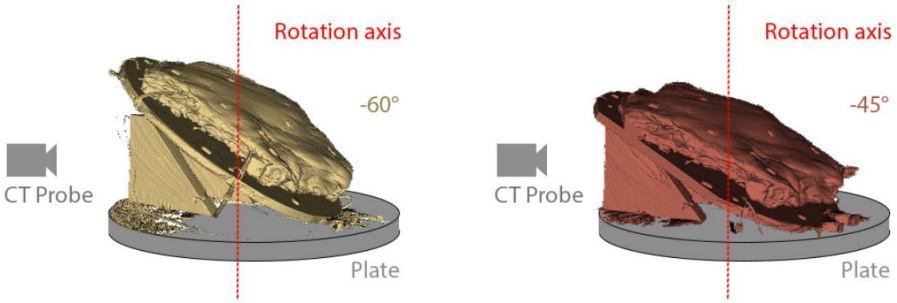

[Lavigne et al., 2022]

Material and Methods

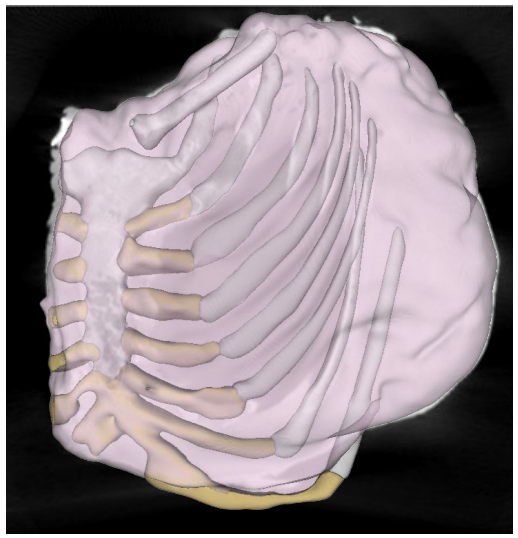

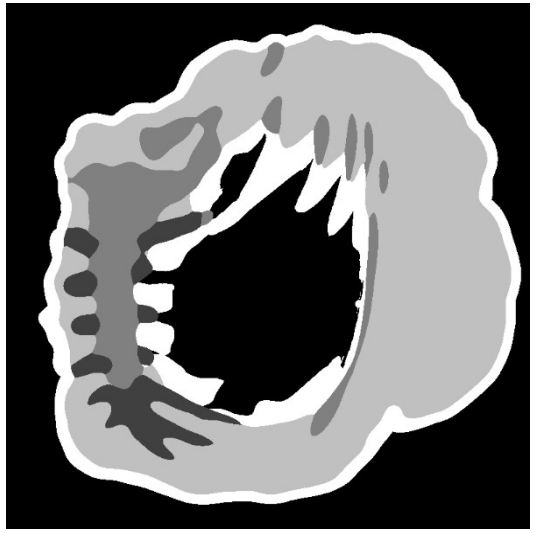

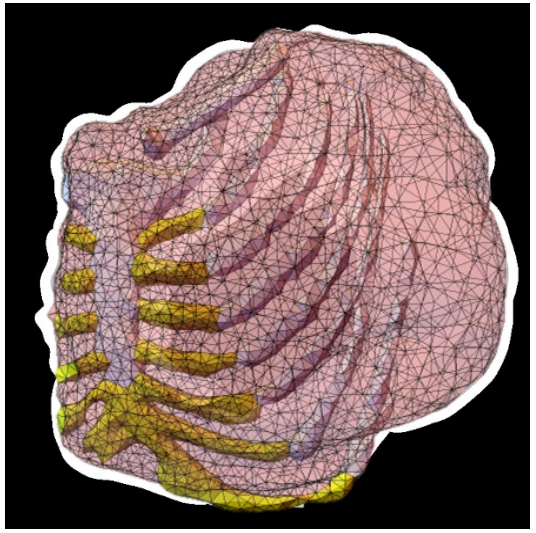

Mesh creation:

- Based on the gray levels, phases are identified
- A mask image is created
- Meshes are courtesy of **Synopsys**

[Lavigne et al., 2022],
[Fedorov et al., 2012]

Material and Methods

Heterogeneous regularised FE-DVC:

Conservation of gray levels: $\Phi_c^2 = \sum_{\text{ROI}} \left(I_0(\boldsymbol{x}) - I_t\left(\boldsymbol{x} + \mathbf{u}(\boldsymbol{x})\right) \right)^2$

[Buljac et al., 2018]

Material and Methods

Heterogeneous regularised FE-DVC:

Conservation of gray levels: $\Phi_c^2 = \sum_{\text{ROI}} \left(I_0(x) - I_t\left(x + \mathbf{u}(x)\right)\right)^2$

Mechanical regularization: $\begin{cases} [\boldsymbol{K}]\{\boldsymbol{v}\} = \{\boldsymbol{f}_{\text{res}}\} \\ \Phi_m^2 = \|\{\boldsymbol{f}_{\text{res}}\}\|^2 = \{\boldsymbol{v}\}^T[\boldsymbol{K}]^T[\boldsymbol{K}]\{\boldsymbol{v}\} \end{cases}$

[Leclerc et al., 2011]

Material and Methods

Heterogeneous regularised FE-DVC:

Conservation of gray levels: $\Phi_c^2 = \sum_{\text{ROI}} \left(I_0(x) - I_t\left(x + \mathbf{u}(x)\right)\right)^2$

Mechanical regularization: $\begin{cases} [\boldsymbol{K}]\{\boldsymbol{v}\} = \{\boldsymbol{f}_{\text{res}}\} \\ \Phi_m^2 = \|\{\boldsymbol{f}_{\text{res}}\}\|^2 = \{\boldsymbol{v}\}^T[\boldsymbol{K}]^T[\boldsymbol{K}]\{\boldsymbol{v}\} \end{cases}$

$$\Phi_{tot}^2 = \Phi_c^2 + w_m \Phi_m^2$$

[Lavigne et al., 2022]

Material and Methods

Heterogeneous regularised FE-DVC:

Elastic **contrast**:

- Eb : 5 to 50 GPa

[Rho et al., 1993; Hunt et al., 1998; Seedhom et al., 2004]

- Ec : 8 to 40 MPa

[Forman and Kent, 2011; Huwe et al., 2018; Griffin et al., 2020]

- Et : 0.2 to 28 kPa

[Payan and Ohayon, 2017; Mîra et al., 2018]

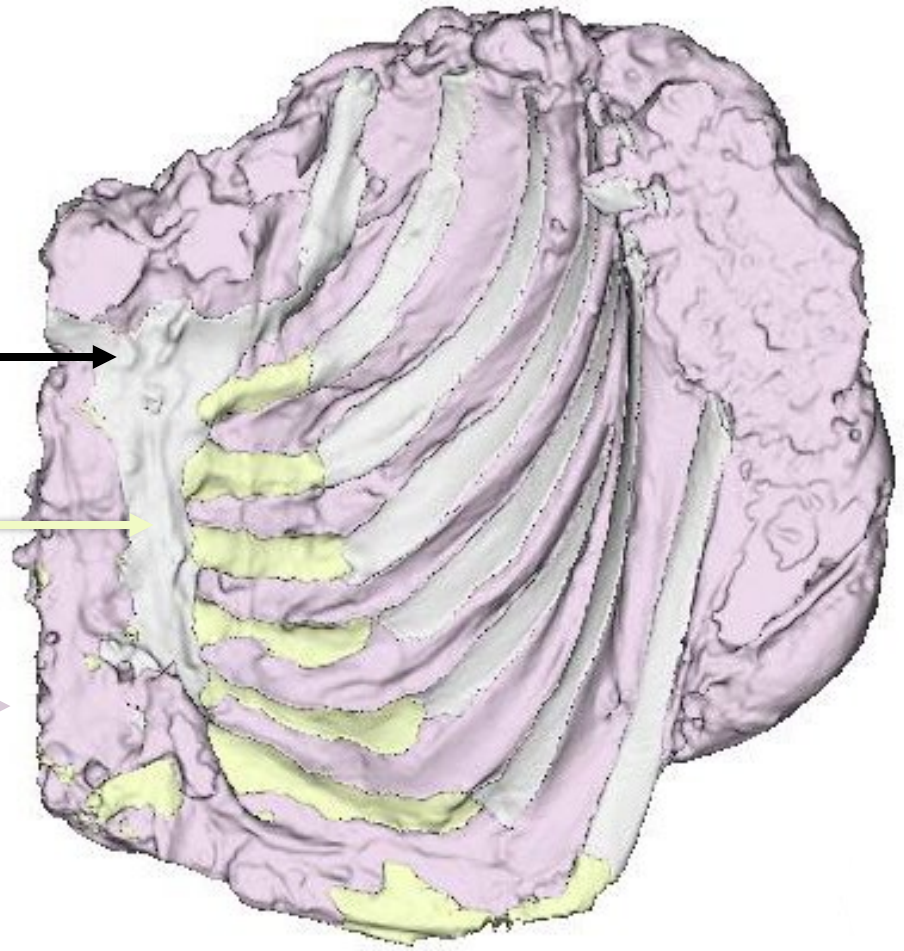

$Cb = 10^6$, $Cc = 10^4$ and $Ct = 1$

Material and Methods

Convergence analysis:

- $\ell reg \leq 3vx$: No convergence for the L^2 norm
- $\ell reg \geq 40$ vx: non-physical regularization & bad conditioning of the DVC Hessian matrix
- $\ell reg = 4vx$ was kept with the highest contrast

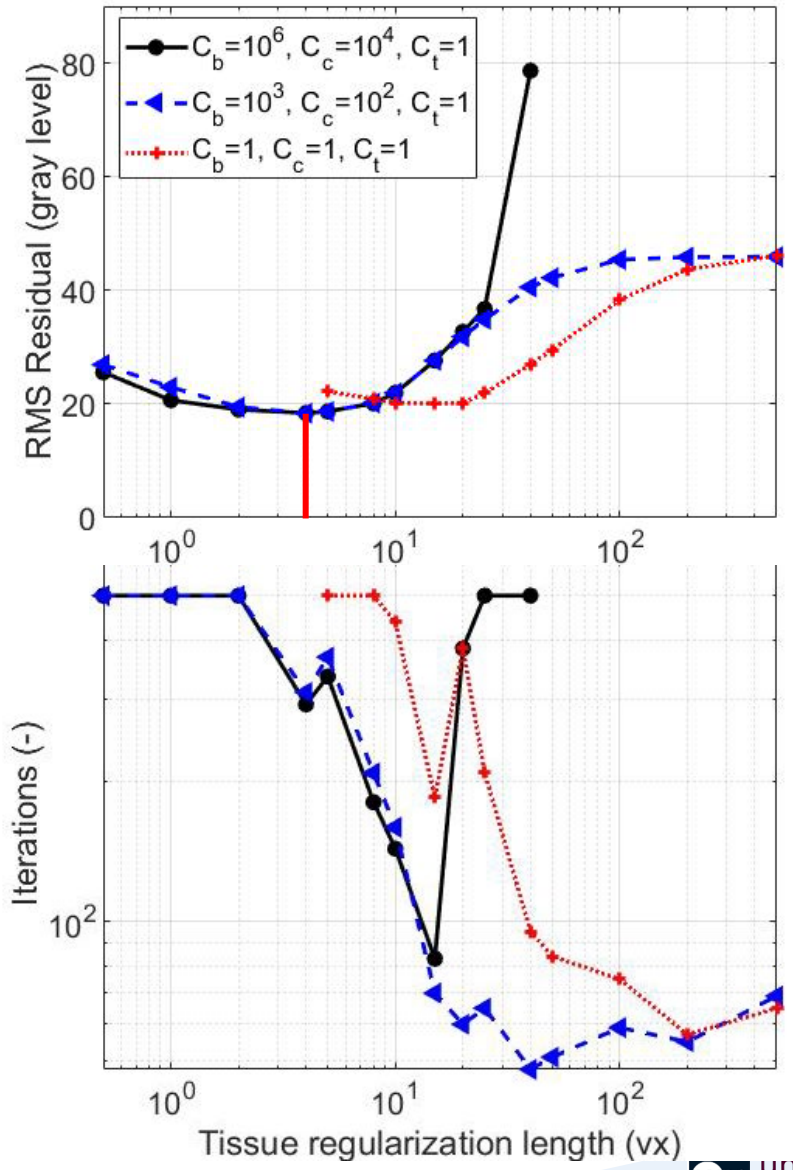

[Lavigne et al., 2022]

Material and Methods

3-step procedure:

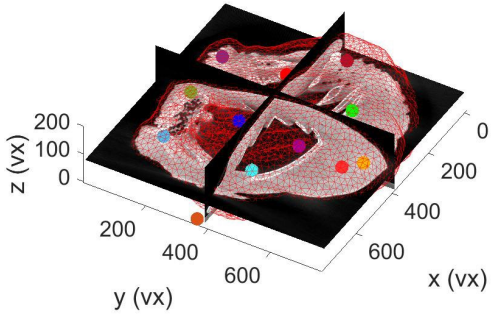

Partial disp. markers

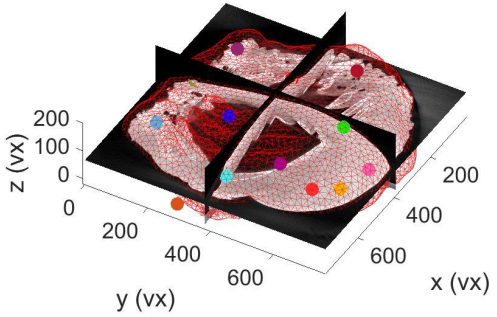

Res = 62.7 GL

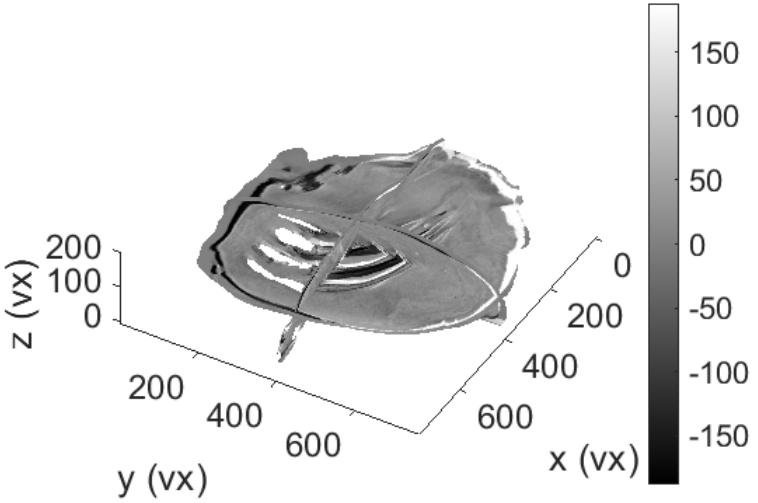

[Lavigne et al., 2022]

Material and Methods

3-step procedure:

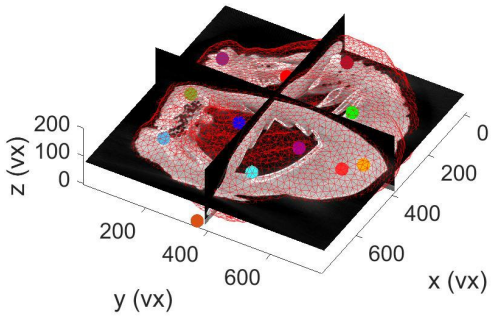

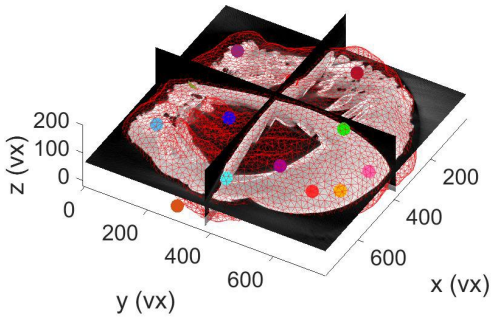

Partial disp. markers

Res = 62.7 GL

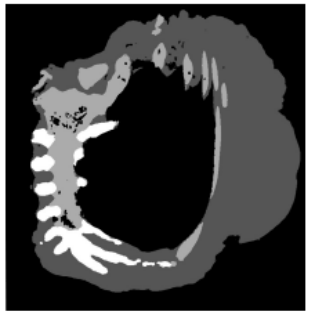

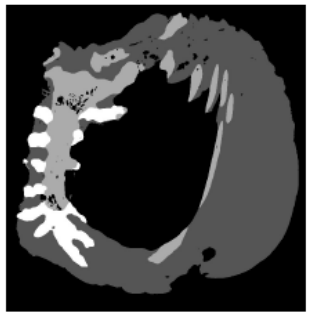

Initial disp. using DVC on masks

Res = 10.6 GL

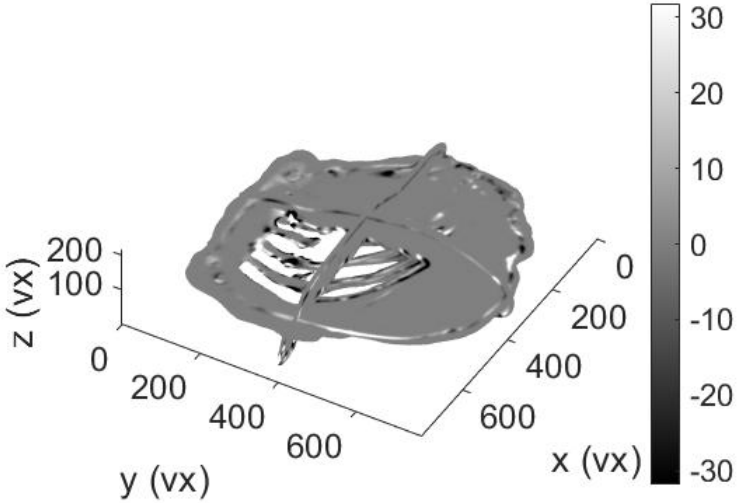

[Lavigne et al., 2022]

Material and Methods

3-step procedure:

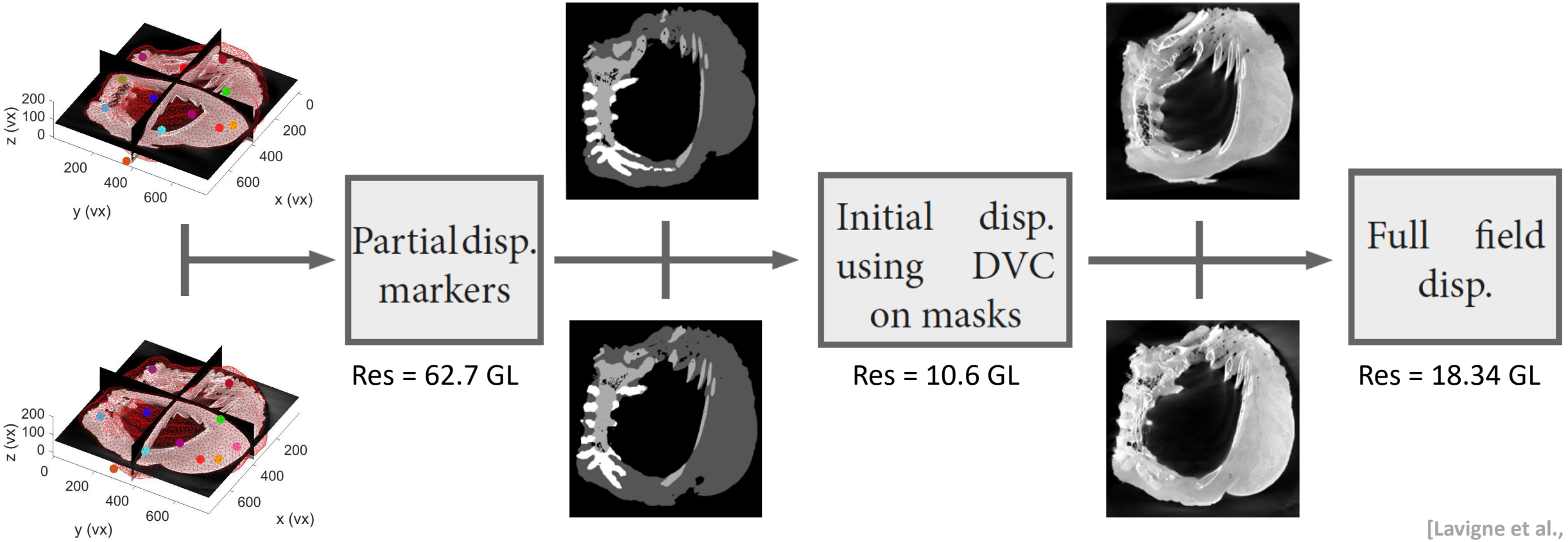

[Lavigne et al., 2022]

Results and Discussion

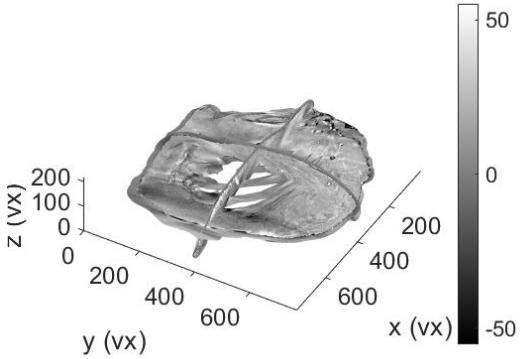

Residuals (gray levels)

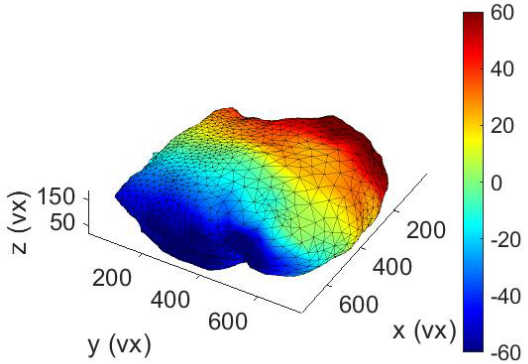

u_x (voxels)

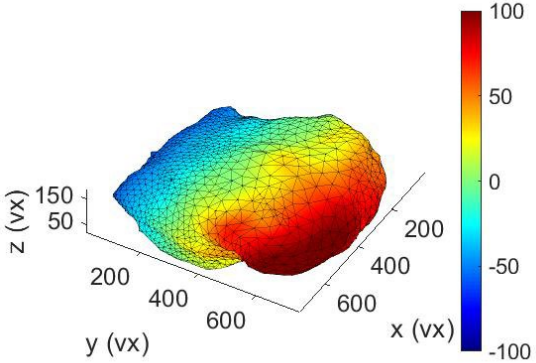

u_y (voxels)

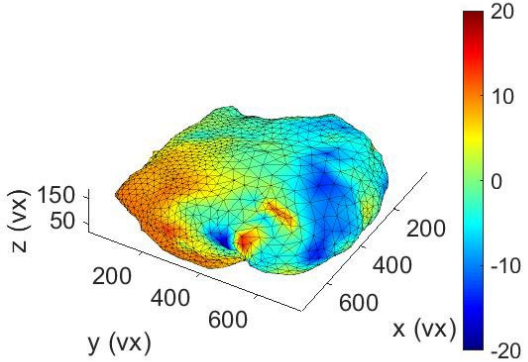

u_z (voxels)

Final RMS residual was 18.3 GL

Displacement includes rigid motion

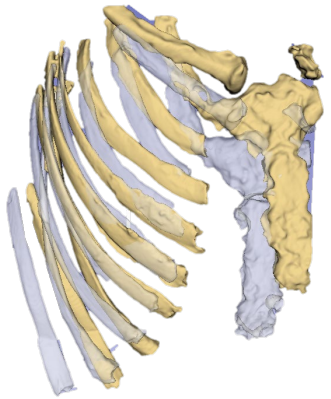

[Lavigne et al., 2022]

Results and Discussion

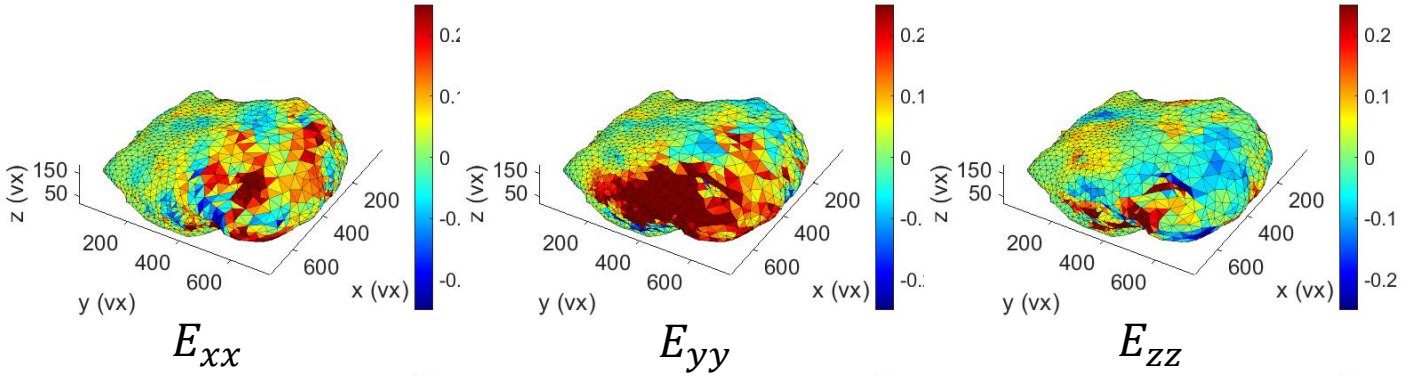

E_{xx} E_{yy} E_{zz}

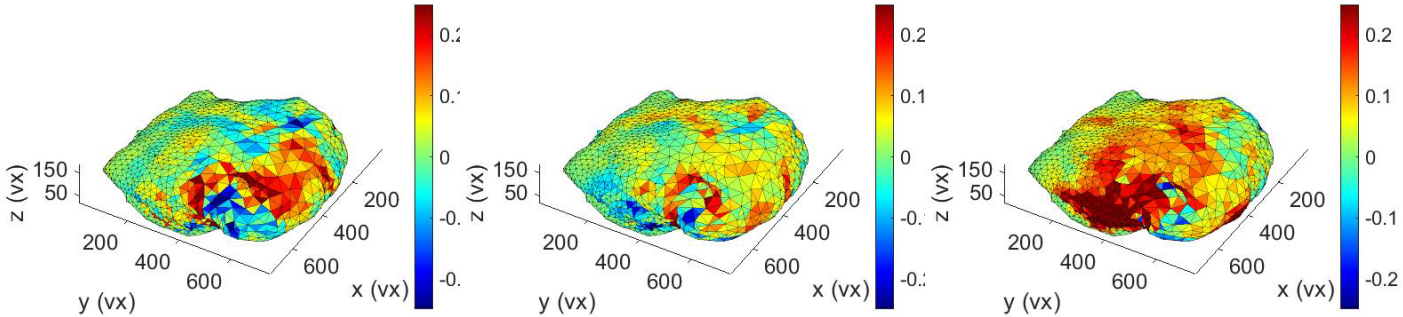

E_{xy} E_{xz} E_{yz}

Green-Lagrange strains:

- Large deformation (>25%)
- Shear in the fold

[Lavigne et al., 2022]

Results and Discussion

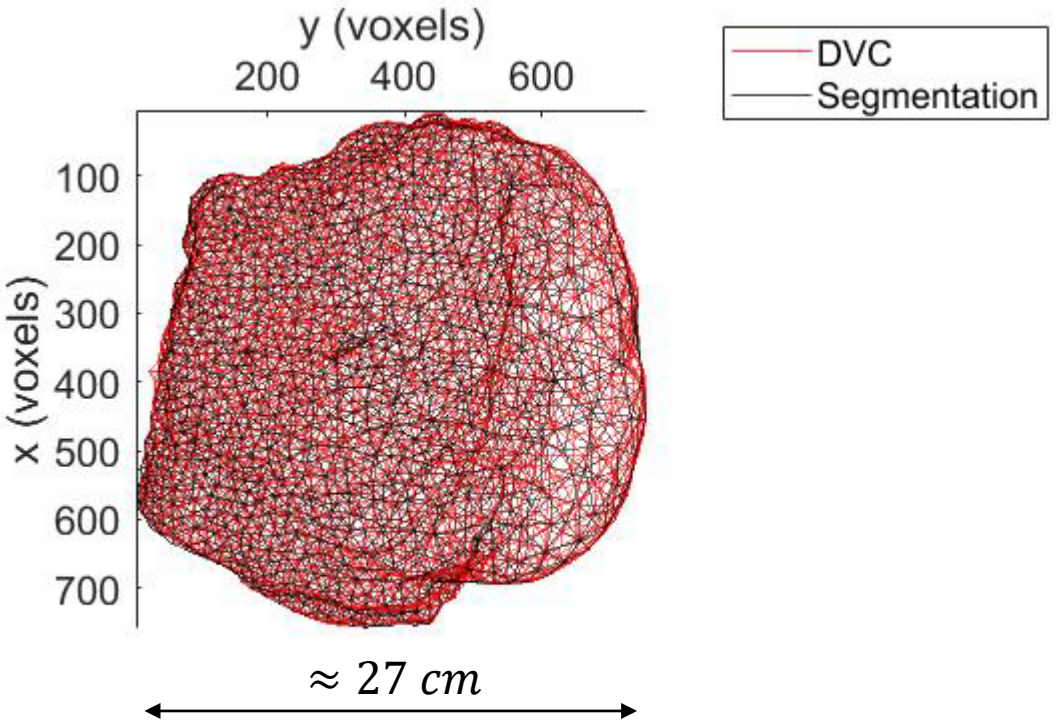

Accurate displacement field (root mean square error <3 mm)

Phase	RMSE (mm)
Soft tissue	2.2 (2.3)
Cartilage	3.1 (3.2)
Bones	2.6 (2.7)

[Lavigne et al., 2022]

Conclusion and limitations

- From **micro-computed tomographies**, computation of the **full field displacement** between 2 complex configurations using **heterogeneous regularized DVC**
- 3-step pipeline has been developed
- The results are deemed trustworthy, supporting the feasibility of its application for breast large deformations

- *Ex-vivo* ≠ *in-vivo* tissues
- Low number of scans and single patient
- Consider body forces
- User uncertainties

Acknowledgments

This study was supported by the European Union's Horizon 2020research and innovation program under grant agreement No 811099, the Marie Skodowska-Curie, Luxembourg grant agreement No. 764644, and the FNR Project No. C20/MS/14782078/QuaC. JL would like to acknowledge the support from EU Horizon 2020 Marie Skodowska Curie Individual Fellowship MOrPhEM under Grant 800150. The medical images used in the present study were obtained at Hopital Arnaud de Villeneuve, Département de Gynécologie Obstétrique in collaboration with Dr. Gauthier Rathat, Prof. Guillaume Captier, and AnatoScope. The authors would like to thank Synopsys for its support in providing access to the Simpleware software to generate the meshes used in this project, and RX-Solutions for their support and answers about the machine settings that were used. Last, the authors sincerely thank the person who donated her body to science so that anatomical research could be performed.

UNIVERSITÉ DU LUXEMBOURG

References

- [Lavigne et al., 2022]: On the Measurement of Breast Deformation via Regularized Digital Volume Correlation.
- [Lavigne et al., 2022]: Implicit inverse hyper-elasticity: identification of material parameters under gravitational loading with contact.
- [Deshpande et al., 2022]: Probabilistic Deep Learning for Real-Time Large Deformation Simulations.
- [Lee et al., 2010]: Breast image registration by combining finite elements and free-form deformations.
- [Gavaghan et al., 2008]: Predicting tumor location by modeling the deformation of the breast.
- [Duraes et al., 2019]: Surgery of nonpalpable breast cancer: First step to a virtual per-operative localization? First step to virtual breast cancer localization.
- [Mazier et al., 2022]: Inverse deformation analysis: an experimental and numerical assessment using the FEniCS Project.
- [Eiben et al., 2016]: Surface driven biomechanical breast image registration.
- [Mazier et al., 2021]: A rigged model of the breast for preoperative surgical planning.
- [Bay et al., 1999]: Digital volume correlation: three-dimensional strain mapping using X-ray tomography.
- [Bay et al., 2008]: Methods and applications of digital volume correlation.
- [Buljac et al., 2018]: Digital volume correlation: Review of progress and challenge.
- [Liu et al., 2007]: Accuracy and precision of digital volume correlation in quantifying displacements and strains in trabecular bone.
- [Benoit et al., 2009]: 3D analysis from micro-MRI during in situ compression on cancellous bone.
- [Leclerc et al., 2011]: Voxel-scale digital volume correlation.
- [Leclerc et al., 2015]: Correli 3.0.
- [Forman and Kent, 2011]: Modeling costal cartilage using local material properties with consideration for gross heterogeneities
- [Huwe et al., 2018]: Characterization of costal cartilage and its suitability as a cell source for articular cartilage tissue engineering.
- [Griffin et al., 2020]: Comparison of thecompressive mechanical properties of auricular and costal cartilage from patientswith microtia.
- [Hussein et al., 2012]: Digital volume correlation for study of the mechanics of whole bone.
- [Gillard et al., 2014]: The application of digital volume correlation (dvc) to study the microstructural behaviour of trabecular bone during compression.
- [Fernandez et al., 2022]: Nonlinear micro finite element models based on digital volume correlation measurements predict early microdamage in newly formed bone.
- [Palanca et al., 2022]: Microfe models of porcine vertebrae with induced bone focal lesions: Validation of predicted displacements with digital volume correlation.
- [Wu et al., 2022]: A combined experimental and numerical method to estimate the elastic modulus of single trabeculae.
- [Santamaria et al., 2020]: Characterization of chemoelastic effects in arteries using digital volume correlation and optical coherence tomography
- [Sartori et al., 2021]: Gaining insight into the deformation of achilles tendon entheses in mice.
- [Disney et al., 2022]: Regional variations in discrete collagen fibre mechanics within intact intervertebral disc resolved using synchrotron computed tomography and digital volume correlation.
- [Disney et al., 2019]: Synchrotron tomography of intervertebral disc deformation quantified by digital volume correlation reveals microstructural influence on strain pattern.
- [Rankin et al., 2020]: Developing an analogue residual limb for comparative dvc analysis of transtibial prosthetic socket design.
- [Pierce et al., 2016]: Novel method to track soft tissue deformation by micro-computed tomography: Application to the mitral valve
- [Fedorov et al. 2012]:3D slicer as an image computing platform for the quantitative imaging network
- [Rho et al., 1993]: Young's modulus of trabecular and cortical bone material: Ultrasonic and micro-tensile measurement
- [Hunt et al., 1998]: Ultrasonic determination of the elastic modulus of human cortical bone
- [Seedhom et al., 2004]: The longitudinal Young's modulus of cortical bone in the midshaft of human femur and its correlation with CT scanning data.
- [Payan and Ohayon, 2017]: Biomechanics of Living Organs: Hyperelastic Constitutive Laws for Finite Element Modeling
- [Mîra et al., 2018]: A biomechanical breast modelevaluated with respect to MRI data collected in three different positions.

This talk takes place in the context of the DRIVEN project funded by the European Union's Horizon 2020 research and innovation programme under grant agreement No 811099 and the Marie Sklodowska-Curie, Luxembourg grant agreement No. 764644.

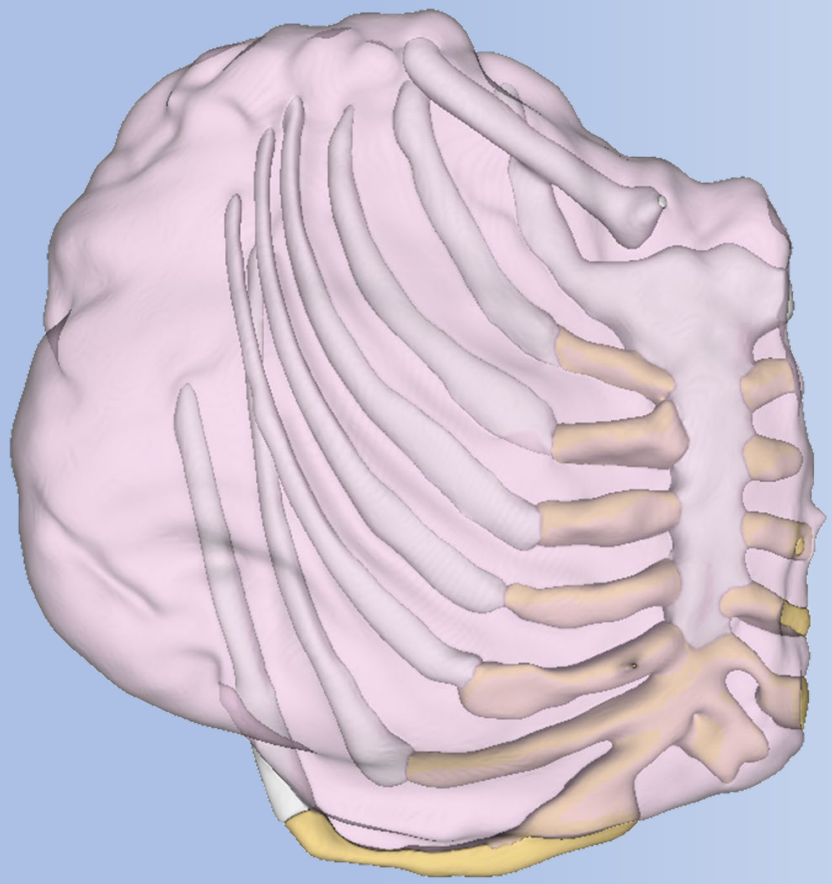

Breast segmentation

Thanks for your attention

Do you have any questions?

European Commission
école normale supérieure paris-saclay
UNIVERSITÉ DU LUXEMBOURG
LMPS université PARIS-SACLAY
RAINBOW Rapid Biomechanics Simulation for Personalized Clinical Design
A Marie Skłodowska-Curie European Training Network
AnatoScope
Legato Team

Appendix: Segmentation

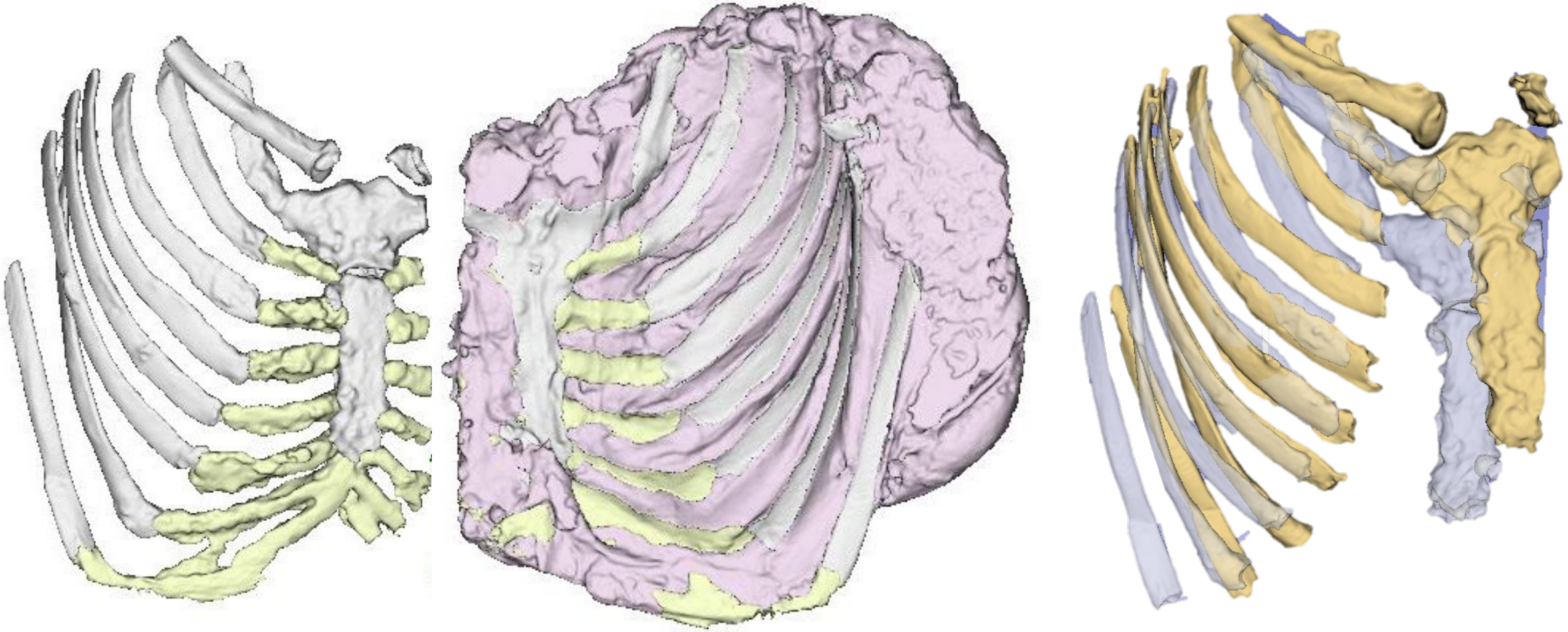

Appendix: DVC hardware parameters

Orientation	−60°	−45°
Tomograph	EasyTom 150 (RX Solution)	EasyTom 150 (RX Solution)
Target/Anode	W (reflection mode)	W (reflection mode)
Voltage	120 kV	120 kV
Current	202 µA	202 µA
Focal spot size	50 µm	50 µm
Tube to detector	610 mm	610 mm
Tube to object	430 mm	430 mm
Detector	Varian 25 × 20 cm	Varian 25 × 20 cm
Definition	1920 × 1536 pixels	1920 × 1536 pixels
Projection definition	1840 × 728 pixels	1840 × 728 pixels
Number of projections	2111	1407
Angular amplitude	360°	360°
Frame average	15 per projection	15 per projection
Frame rate	30 fps	30 fps
Acquisition duration	28 min 08 s	18 min 40 s
Reconstruction algorithm	Filtered back-projection	Filtered back-projection
Filter	Tukey (75%)	Tukey (0%)
Gray levels amplitude	8 bits	8 bits
Volume size	768 × 781 × 216 voxels (after crop)	768 × 781 × 216 voxels (after crop)
Field of view	261.12 × 265.54 × 73.44 mm^3 (after crop)	261.12 × 265.54 × 73.44 mm^3 (after crop)
Image scale	0.34 mm/voxel	0.34 mm/voxel

Appendix: Breast DVC convergence

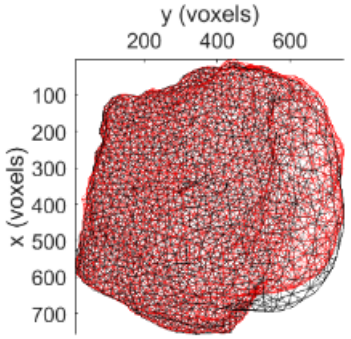

(a) ℓ_{reg}=500 vx

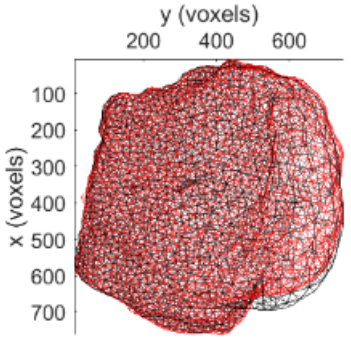

(b) ℓ_{reg}=200 vx

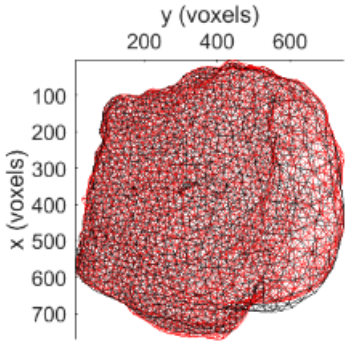

(c) ℓ_{reg}=100 vx

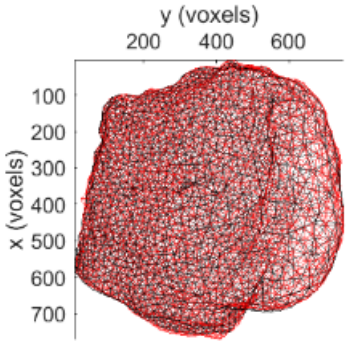

(d) ℓ_{reg}=50 vx

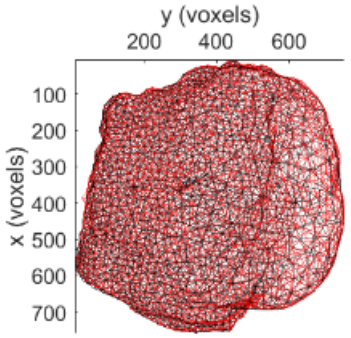

(e) ℓ_{reg}=20 vx

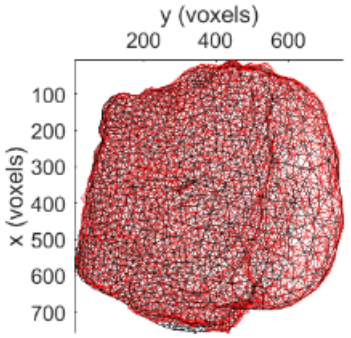

(f) ℓ_{reg}=5 vx

Appendix: Breast DVC results

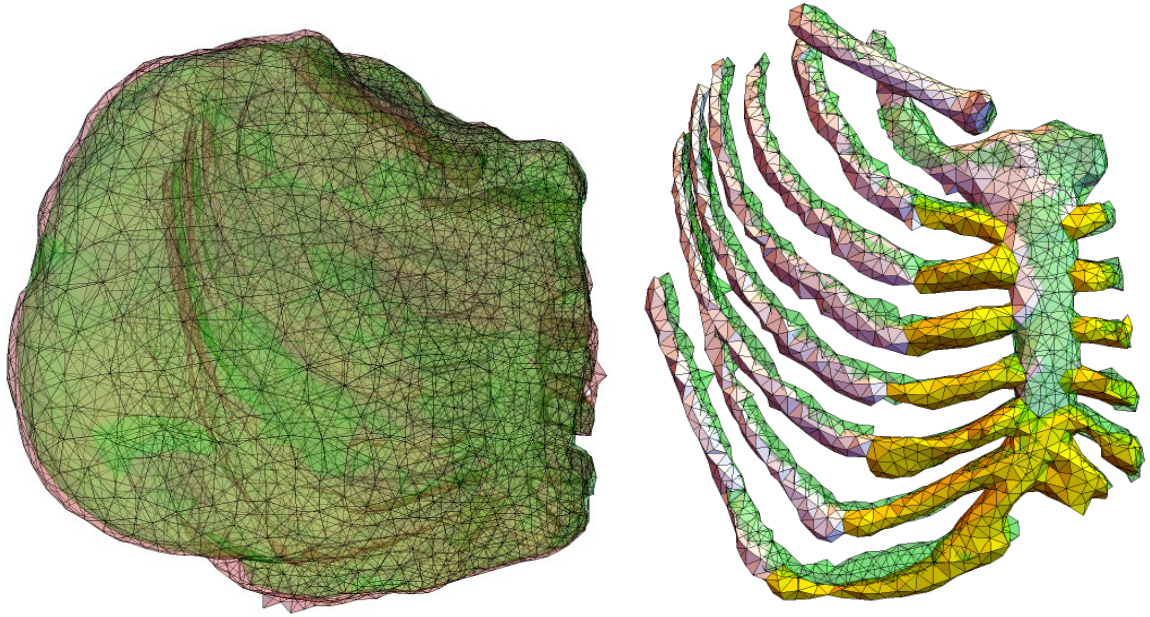

DVC applied to -60° configuration (green) and segmentation in -45°

$$\mathrm{RMSE}^2 = \frac{1}{N}\sum_{i=1}^{N}\left(\mathbf{x_i}^{\mathrm{DVC}} - \mathcal{P}^{seg}\left(\mathbf{x_i}^{\mathrm{DVC}}\right)\right)^2$$

Phase	RMSE (mm)
Soft tissue	2.31
Cartilage	3.18
Bones	2.72

Appendix: Gravity identification

$$\tilde{\mathbf{g}} = \begin{pmatrix} 0 \\ -9.81 \\ 0 \end{pmatrix}_{(X_m,\ Y_m,\ Z_m)}$$

$$\mathbf{R_x} = \begin{pmatrix} 1 & 0 & 0 & 0 \\ 0 & cos(\theta_x) & -sin(\theta_x) & 0 \\ 0 & sin(\theta_x) & cos(\theta_x) & 0 \\ 0 & 0 & 0 & 1 \end{pmatrix}_{(X_m,\ Y_m,\ Z_m)}$$

$$\mathbf{R_y} = \begin{pmatrix} cos(\theta_y) & 0 & sin(\theta_y) & 0 \\ 0 & 1 & 0 & 0 \\ -sin(\theta_y) & 0 & cos(\theta_y) & 0 \\ 0 & 0 & 0 & 1 \end{pmatrix}_{(X_m,\ Y_m,\ Z_m)}$$

$$\mathbf{R_z} = \begin{pmatrix} cos(\theta_z) & -sin(\theta_z) & 0 & 0 \\ sin(\theta_z) & cos(\theta_z) & 0 & 0 \\ 0 & 0 & 1 & 0 \\ 0 & 0 & 0 & 1 \end{pmatrix}_{(X_m,\ Y_m,\ Z_m)}$$

$$\mathbf{T} = \begin{pmatrix} 1 & 0 & 0 & t_x \\ 0 & 1 & 0 & t_y \\ 0 & 0 & 1 & t_z \\ 0 & 0 & 0 & 1 \end{pmatrix}_{(X_m,\ Y_m,\ Z_m)}$$

$$\tilde{\mathbf{P}} = \mathbf{R_z} \cdot \mathbf{R_y} \cdot \mathbf{R_x} \cdot \mathbf{T} \cdot \mathbf{P}$$

$$\mathbf{g} = (\mathbf{R_z} \cdot \mathbf{R_y} \cdot \mathbf{R_x} \cdot \mathbf{T})^{-1} \cdot \tilde{\mathbf{g}}$$

$$\Leftrightarrow \mathbf{g} = \mathbf{T}^{-1} \cdot \mathbf{R_x}^{\mathrm{T}} \cdot \mathbf{R_y}^{\mathrm{T}} \cdot \mathbf{R_z}^{\mathrm{T}} \cdot \tilde{\mathbf{g}}$$

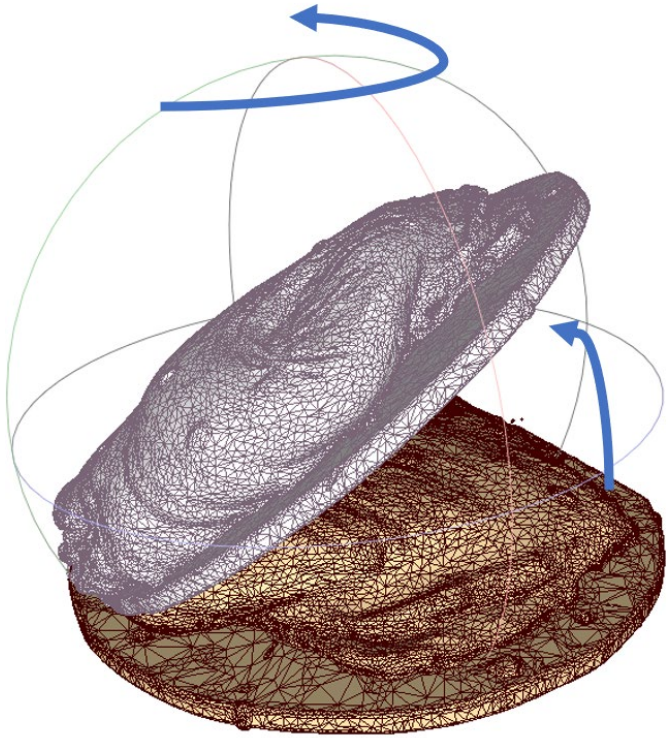

Appendix: Uncertainty quantification

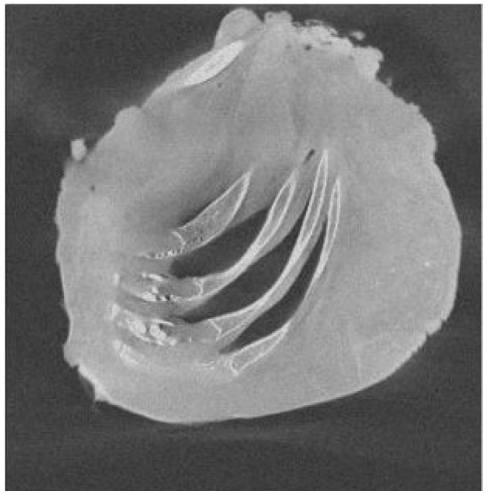

Uncertainty evaluation

- White Gaussian noise was added to the translated reference volume.
- Registering to the reference volume.
- Displacement uncertainties = standard deviations of nodal displacements.
- Regularized DVC => the fine mesh was not altered but the regularization length ℓreg was varied [Leclerc et al., 2011; Taillandier-Thomas et al., 2014].

[Lavigne et al., 2022]

Appendix: Uncertainty quantification

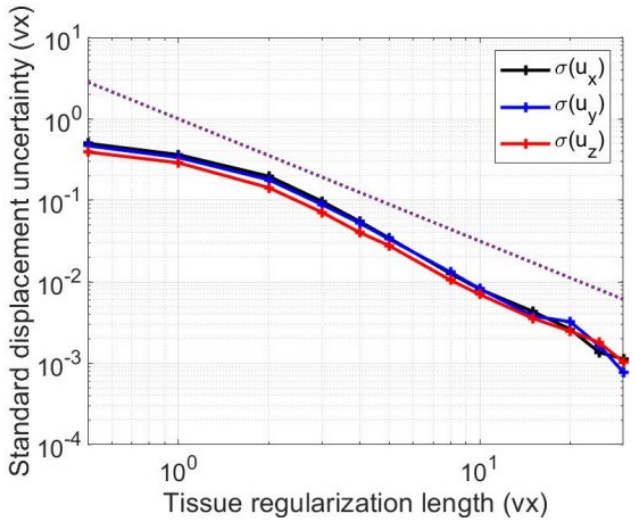

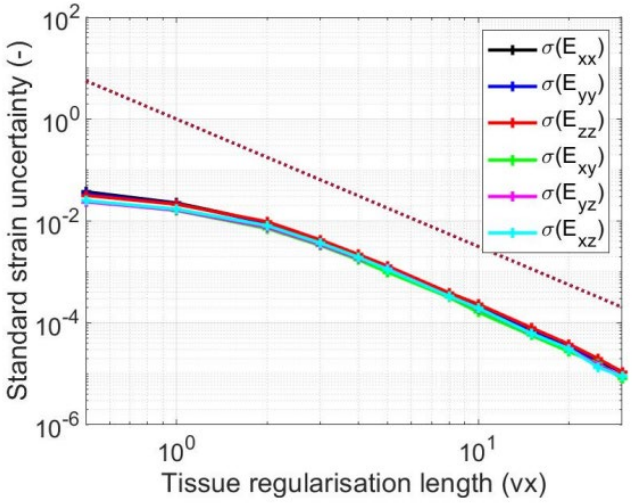

Uncertainty evaluation

- The displacement power law interpolation with exponent −1.5 corresponding to Gaussian noise is recovered
- The strain power law interpolation with exponent −2.5 corresponding to Gaussian noise is recovered
- 4vx regularization length leads to 0.1vx displacement uncertainty, which is acceptable given the previous results.

[Lavigne et al., 2022]

Appendix: Parameter identification FE framework

Input: 2 loaded configurations

(2 benchmark problems)

Inverse-forward FE model

(Neo-Hookean law & contact)

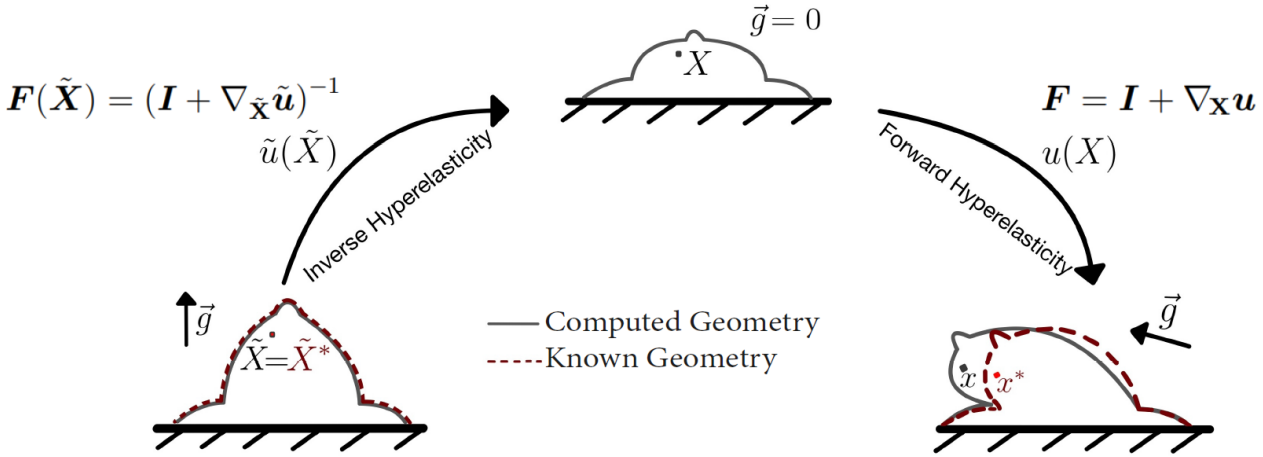

[Lavigne et al., 2022]